JOURNAL OF BACTERIOLOGY, Nov. 2007, p. 8179–8185 Vol. 189, No. 22
0021-9193/07/$08.00+0 doi:10.1128/JB.00479-07

Characterization and Comparison of Biofilm Development by Pathogenic and Commensal Isolates of *Histophilus somni*▽

Indra Sandal,[1] Wenzhou Hong,[2] W. Edward Swords,[2] and Thomas J. Inzana[1]*

Center for Molecular Medicine and Infectious Diseases, Virginia-Maryland Regional College of Veterinary Medicine, Virginia Polytechnic Institute and State University, Blacksburg, Virginia,[1] and Department of Microbiology and Immunology, Wake Forest University Health Sciences, Winston-Salem, North Carolina[2]

Received 29 March 2007/Accepted 12 July 2007

***Histophilus somni* (*Haemophilus somnus*) is an obligate inhabitant of the mucosal surfaces of bovines and sheep and an opportunistic pathogen responsible for respiratory disease, meningoencephalitis, myocarditis, arthritis, and other systemic infections. The identification of an exopolysaccharide produced by *H. somni* prompted us to evaluate whether the bacterium was capable of forming a biofilm. After growth in polyvinyl chloride wells a biofilm was formed by all strains examined, although most isolates from systemic sites produced more biofilm than commensal isolates from the prepuce. Biofilms of pneumonia isolate strain 2336 and commensal isolate strain 129Pt were grown in flow cells, followed by analysis by confocal laser scanning microscopy and scanning electron microscopy. Both strains formed biofilms that went through stages of attachment, growth, maturation, and detachment. However, strain 2336 produced a mature biofilm that consisted of thick, homogenous mound-shaped microcolonies encased in an amorphous extracellular matrix with profound water channels. In contrast, strain 129Pt formed a biofilm of cell clusters that were tower-shaped or distinct filamentous structures intertwined with each other by strands of extracellular matrix. The biofilm of strain 2336 had a mass and thickness that was 5- to 10-fold greater than that of strain 129Pt and covered 75 to 82% of the surface area, whereas the biofilm of strain 129Pt covered 35 to 40% of the surface area. Since *H. somni* is an obligate inhabitant of the bovine and ovine host, the formation of a biofilm may be crucial to its persistence in vivo, and our in vitro evidence suggests that formation of a more robust biofilm may provide a selective advantage for strains that cause systemic disease.**

Bacterial biofilms are aggregations of bacteria that live in a highly structured and organized community. Biofilms typically become established by attachment of planktonic cells to a surface, followed by production of an extracellular polymeric substance (ePS) that may consist of polysaccharide, proteins, and nucleic acids. This interconnecting matrix links the bacterial cells together and begins the establishment of an organized community. As this congregation of cells matures, it develops into a well-organized biofilm, which has a distinct architecture containing open water channels that provide oxygen and nutrients to embedded cells (39, 44). This organization enables the bacteria to live as a community at a site they could not otherwise colonize as planktonic cells. Biofilms have long been recognized in extreme environmental settings (39) and are now recognized as important complicating factors in many bacterial infections, including mitral valve endocarditis, osteomyelitis, dental caries, middle-ear infections, medical device-related infections, and respiratory disease due to cystic fibrosis (11). A biofilm enhances the resistance of the bacteria to treatment with antibiotics and host defense mechanisms and enables the bacteria to colonize a host site that is difficult to later eradicate.

Histophilus somni (*Haemophilus somnus*) is a gram-negative coccobacillus and member of the *Pasteurellaceae* (3). It is a host-specific opportunistic pathogen of cattle and sometimes sheep. *H. somni* is one of the pathogens responsible for bovine respiratory disease complex, which is responsible for 61.5% of the mortality in North American feedlot cattle, as well as decreased weight gain and morbidity in an additional 10% of these animals (34). In addition to pneumonia (2, 13, 21), *H. somni* can cause meningoencephalitis, myocarditis, arthritis, septicemia, and other systemic infections (7, 22). *H. somni* expresses a wide array of virulence factors, including phase variation of lipooligosaccharide epitopes (20, 24, 25, 52), decoration of lipooligosaccharide with sialic acid and phosphorylcholine (20, 24, 43), expression of high-molecular-weight immunoglobulin-binding proteins (5, 6, 51), intracellular survival in professional phagocytes (8, 33), and induction of apoptosis (46, 47). However, urogenital strains of *H. somni* lack many of these virulence factors and are incapable or less capable of causing disease than isolates from normally sterile sites (43). Recent genome sequencing of urogenital isolate strain 129Pt (4) and pneumonia isolate strain 2336 (42) identified many genetic differences responsible for some of these virulence attributes. Although clinical isolates of *H. somni* are phenotypically very similar, strains can be classified by ribotyping (14) and other molecular methods such as PCR (48).

Although many pathogenic members of the family *Pasteurellaceae* are encapsulated (32, 36, 37), a capsule has not been identified on the surface of *H. somni*. However, we have described the production of an exopolysaccharide (22), which is a common component of bacterial biofilms. Therefore, we sought to determine whether *H. somni* produced a biofilm and, if so, characterize the formation of this biofilm by pathogenic

* Corresponding author. Mailing address: Center for Molecular Medicine and Infectious Diseases, Virginia-Maryland Regional College of Veterinary Medicine, Virginia Polytechnic Institute and State University, 1800 Kraft Dr., Suite 200, Blacksburg, VA 24061. Phone: (540) 231-4692. Fax: (540) 231-5553. E-mail: tinzana@vt.edu.

▽ Published ahead of print on 20 July 2007.

and commensal strains. We now describe a comprehensive investigation of biofilm development by *H. somni* and show that pathogenic and commensal strains display very diverse phenotypes at different stages in biofilm development. The implication of such biofilm development by this obligate inhabitant of bovine mucosal surfaces is discussed.

MATERIALS AND METHODS

Bacteria and culture conditions. *H. somni* strain 2336 (a pathogenic, pneumonia isolate), strain 129Pt (a commensal isolate from the bovine prepuce) and other *H. somni* strains were provided and have been characterized by Lynette Corbeil (University of California at San Diego) (6). Additional *H. somni* clinical isolates were obtained from necropsy specimens and were provided by Andrew Potter (Veterinary Infectious Disease Organization, Saskatoon, Saskatchewan, Canada). These isolates were identified as *H. somni* by standard biochemical and phenotypic tests at the Animal Health Laboratory at the Animal Health Division of Alberta Agriculture (Edmonton, Alberta, Canada). *H. somni* was propagated from −80°C skim milk stock cultures onto Columbia agar containing 5% sheep blood and incubated at 37°C in 5% CO2. Colonies from 36-h cultures were inoculated into brain heart infusion (BHI) broth supplemented with 0.1% Trizma base and 0.01% thiamine monophosphate (BHI-TT) (23) and shaken at 200 rpm at 37°C to late-log phase (5×10^9 CFU/ml) for growth of planktonic cells. *Actinobacillus pleuropneumoniae* strains J45 and K17 and nonencapsulated mutants of these strains have been previously described (26, 27). *A. pleuropneumoniae* serotype 7 strains 29628 and 5372/96 were obtained from Martha Mulks (Michigan State University, East Lansing, MI) and from Karen Post (Rollins Diagnostic Laboratory, Raleigh, NC), respectively. Biofilm-producing strains of *Pseudomonas aeruginosa* were provided by Joanna Goldberg (University of Virginia, Charlottesville), and *Haemophilus influenzae* type b strain Eag was provided by Porter Anderson (University of Rochester School of Medicine, Rochester, NY). *Haemophilus parasuis* strain 8869/92 and *Mannheimia haemolytica* A1 were provided by Karen Post and Reggie Lo (University of Guelph, Guelph, Ontario, Canada), respectively. Strains of *H. parasuis* and *A. pleuropneumoniae* were grown in BHI supplemented with 5 μg of NAD/ml, and *H. influenzae* was grown in the same medium also supplemented with 5 μg of hemin/ml. All other strains were grown in BHI only.

Biofilm assay in PVC wells. *H. somni* strains were grown overnight in 10 ml of BHI-TT, diluted 1:100 in the same medium, and 100 μl of diluted culture was transferred in triplicate to 96-well, polyvinyl chloride (PVC) microtiter wells (Falcon 3911, Microtest III flexible assay plate; Becton Dickinson). The samples were incubated at 37°C for 48 h, and 25 μl of 1% crystal violet was added to each well. After 15 min, the wells were washed three times with sterile distilled water. The biofilm formed in the PVC wells was quantified by addition of 95% alcohol to solubilize the crystal violet, and the absorbance at 630 nm was determined.

Biofilm formation in flow cells. Single chamber flow cells (Stovall Life Science, Inc., Greensboro, NC) were obtained as sterile units and assembled according to the manufacturer's instructions. The chamber of the flow cell was inoculated with 6 to 8 ml of *H. somni* strains 2336 or 129Pt in late log phase (5×10^9 CFU/ml). After inoculation, the medium flow was arrested for 3 h, and the flow cell was inverted to enable adhesion of the bacteria to the flow cell coverslip. Medium flow was resumed at a constant rate of 0.33 ml/min using a peristaltic pump (Cole Parmer, Vernon Hills, IL). The continuous-flow cell system was incubated at 37°C for 1, 3, 5, and 7 days. Effluent from the flow cell was collected and cultured to confirm lack of contamination. Each experiment was repeated twice with both strains at the same time intervals.

CLSM. For 3-dimensional analysis of biofilms, confocal laser scanning microscopy (CLSM) was performed by using a Zeiss LSM 510 laser scanning microscope mounted on an Axiovert 100M apparatus (Carl Zeiss, Jena, Germany) with a Fluar 20×/0.75UV objective. The LSM image browser software was used for analysis of biofilm images, which allowed for collection of z-stacks, three-dimensional reconstruction, collection of time series, and data analysis. Images were acquired from random positions in the upper part of the flow cell at 4-μm intervals through the biofilm. The number of images in each stack varied based on the thickness of the biofilm. Each image stack consisted of 60 to 90 images for *H. somni* strain 2336 and 8 to 20 images for *H. somni* strain 129Pt, since the biofilm thickness of strain 129Pt was too low to obtain more images under similar conditions.

After 1, 3, 5, and 7 days of continuous-flow incubation the flow cell chamber was opened, the upper flow cell portion with the coverslip containing the biofilm was washed with phosphate-buffered saline (pH 7.2) (PBS), and LIVE/DEAD BacLight stain (bacterial viability staining kit; Molecular Probes, Inc., Eugene, OR) was added. After 15 min of incubation at room temperature in the dark the coverslips were washed in PBS and visualized by CLSM. COMSTAT software (The Math Works, Inc., Natick, MA) was used to quantify the three-dimensional biofilm images acquired by CLSM (18). Measurements of the biomass, maximum thickness, mean thickness, roughness, substratum coverage, and surface/volume ratio were chosen to characterize the biofilm structures developed by both *H. somni* strains.

SEM. The lower portion of the flow cell containing the coverslip was washed with PBS three times and fixed using 2.5% glutaraldehyde in PBS for 60 min. The coverslips were then rinsed twice for 10 min each in PBS and processed for scanning electron microscopy (SEM) by using a graded acetone dehydration series, followed by the addition of osmium tetraoxide (19). The samples were subjected to critical drying, mounted onto stubs, and coated with palladium. The specimens were viewed on a Phillips SEM-515 scanning electron microscope, and images were obtained at various levels of magnification.

Statistical analysis. The statistical significance (*P* value) of data obtained using the COMSTAT software was determined by a paired, one-tailed *t* test using GraphPad Prism version 4.0 (GraphPad Software, San Diego, CA.). The LSM software package (Carl Zeiss) was used to show the substratum coverage and mean thickness of *H. somni* strains 2336 and 129Pt at the time intervals of 1, 3, 5, and 7 days of growth.

RESULTS

Biofilm formation by *H. somni* in PVC wells. As a screen for biofilm formation, *H. somni* and control strains were grown in PVC wells under stationary conditions at 37°C. *H. somni* strain 129Pt formed quantitatively less biofilm than strain 2336 after 48 h of incubation (lanes 2 and 3, Fig. 1A). In contrast, *H. influenzae* type b strain Eag, *A. pleuropneumoniae* strains 29628, 5372/96, J45 serotype 5, and its isogenic nonencapsulated mutant, *H. parasuis* strain 8869/92, and *M. haemolytica* A1 formed no biofilm in this assay. However, *P. aeruginosa* and *A. pleuropneumoniae* strain K17 serotype 5 did form a biofilm, but the nonencapsulated mutant of strain K17 did not (Fig. 1A). All strains of *H. somni* tested formed some biofilm in PVC wells. However, when the amount of crystal violet-stained biofilm was quantified, it was found that the majority of disease isolates formed more biofilm than commensal isolates from the healthy bovine prepuce (lanes 5 to 8 represent results from the preputial isolates, and lanes 9 to 52 represent results from the disease isolates) (Fig. 1B).

Biofilm formation by *H. somni* in a continuous-flow cell. Pathogenic strain 2336 and commensal strain 129Pt were chosen for biofilm analysis because these strains have been well characterized and both of their genomes have been sequenced (4, 12). The morphological features of the mature biofilms of both strains were examined after growth in a continuous-flow cell system, followed by CLSM, SEM, and topographical analysis. The biofilms were categorized into four distinct stages after 7 days of growth. The stages (Fig. 2) corresponded to periods of (i) attachment, (ii) growth, (iii) maturation, and (iv) detachment. At stage 1 (1-day-old biofilm), the bacterial cells attached to the surface and formed small cell aggregations. The biofilms of both strains 2336 (Fig. 2A1) and 129Pt (Fig. 2B1) consisted of a sparse single layer of cells. However, small cell clusters and aggregates were seen in greater number in strain 2336 (Fig. 2C1 and 2E1) than in strain 129Pt (Fig. 2D1 and 2F1).

During stage 2 (3-day-old biofilm) there was early development of biofilm architecture, and cell clusters gradually increased in size and number. Strain 2336 formed a thick structure (Fig. 2A2 and 2E2) with large numbers of microcolonies associated with opaque extracellular matrix strands (Fig. 2C2).

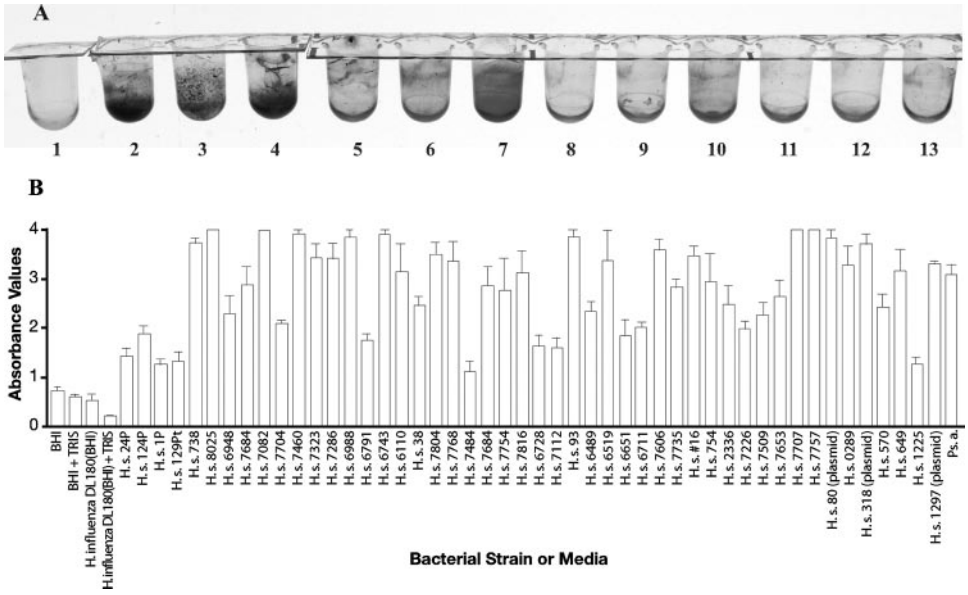

FIG. 1. Biofilm formation by *H. somni* and control strains in PVC wells. (A) Bacteria or medium alone were incubated in PVC wells for 48 h at 37°C prior to staining with crystal violet. Lanes: 1, BHI; 2, *H. somni* strain 2336; 3, *H. somni* strain 129Pt; 4, *P. aeruginosa*; 5, *H. influenzae* type b; 6, *A. pleuropneumoniae* strain 29628 serotype 7; 7 and 8, *A. pleuropneumoniae* K17 serotype 5 and its nonencapsulated mutant, respectively; 9 and 10, *A. pleuropneumoniae* J45 serotype 5 and its nonencapsulated mutant, respectively; 11, *A. pleuropneumoniae* strain 5372/96; 12, *M. haemolytica* A1; and 13, *H. parasuis* 8869/92. (B) Biofilm quantification by different strains of *H. somni* after growth in BHI-TT in PVC wells, crystal violet staining, ethanol solubilization, and determination of the absorbance at 630 nm. Bars represent the means of three independent experiments performed in triplicate. Error bars represent the standard deviations. The *y* axis is the optical density at 630 nm.

However, strain 129Pt formed thin, elongated cell clusters extending from smaller microcolonies (Fig. 2B2 and 2F2) that were attached by thin strands of extracellular matrix (Fig. 2D2).

At stage 3 (5-day-old biofilm), the biofilm had fully matured, and the microcolonies reached maximum size with a complex architecture. The biofilm of strain 2336 was highly structured (Fig. 2A3 and 2E3) with numerous microcolonies encased in a thick, amorphous, and opaque extracellular matrix with water channels (Fig. 2C3 and 2E3). In contrast, strain 129Pt formed various types of cell clusters (Fig. 2B3 and 2F3), some of which turned into distinct tower-shaped structures intertwined with each other by strands of ePS matrix (Fig. 2D3).

At stage 4 (7-day-old biofilm), the large microcolonies began to separate, with disruption of the complex structure of the biofilms. The biofilm of strain 2336 appeared flat, smaller in size with less matrix (Fig. 2A4 and 2E4), and with new cell formations (Fig. 2C4); planktonic cells were seen in various phases of dispersion. Similar features were noted in strain 129Pt, in which the biofilm was also reduced in size (Fig. 2B4 and 2F4). The resulting structure was stretched and disrupted (Fig. 2D4), with dispersion of planktonic cells.

The bacterial LIVE/DEAD stain was used for staining biofilms for CLSM. On days 1 and 3, live organisms (green) were predominant throughout the biofilm, compared to dead organisms (red) (Fig. 2A2 and 2B2). In contrast, on days 5 and 7, the proportion of live organisms appeared to decrease, whereas the number of dead organisms increased throughout the biofilm (Fig. 2A3, 2B3, 2A4, and 2B4). This suggested that in the continuous-flow system, *H. somni* biofilms formed new developmental stages, each of which appeared to have a limited life span. Of note, the intense red fluorescence in biofilm at day 5 (Fig. 2A3 and 2B3) may be a false depiction of the number of dead cells and may be due to the presence of extracellular double-stranded DNA present in the biofilm matrix, as shown by Jurcisek and Bakaletz in a nontypeable strain of *H. influenzae* (29).

Overall, biofilm formation in strains 2336 and 129Pt occurred in a chronological process of initial attachment of cells to a substratum, formation of cell clusters embedded in a matrix of ePS, biofilm maturation, and finally disruption of the complex structure (Fig. 2).

Quantitative analysis of biofilm architecture. To confirm the CLSM observations of biofilm structure, the COMSTAT image analysis program was used to evaluate six variables of biofilm architecture: total biomass, average thickness, maximum thickness, roughness coefficient, surface to volume ratio, and substratum coverage (Fig. 3). Each of these variables was significantly different between strains 2336 and 129Pt ($P = 0.02$ to 0.04).

At day 1, the mean thickness, biomass, and substratum coverage of the biofilms in strains 2336 and 129Pt was low and the surface-to-volume ratio was high, which was evidence that the cells and cell clusters had attached to the substratum. Single cells and small cell clusters have a greater surface to volume ratio than larger microcolonies. However, there were more cell clusters and aggregates formed by strain 2336 than by strain 129Pt. The biomass and mean thickness of the biofilm of strain 2336 were 10 $\mu m^3/\mu m^2$ and 12 to 15 μm, respectively, whereas the same parameters for strain 129Pt were 1.04 $\mu m^3/\mu m^2$ and 0.8 to 1 μm, respectively (Fig. 3A and B).

At day 3, small microcolonies and cell clusters had devel-

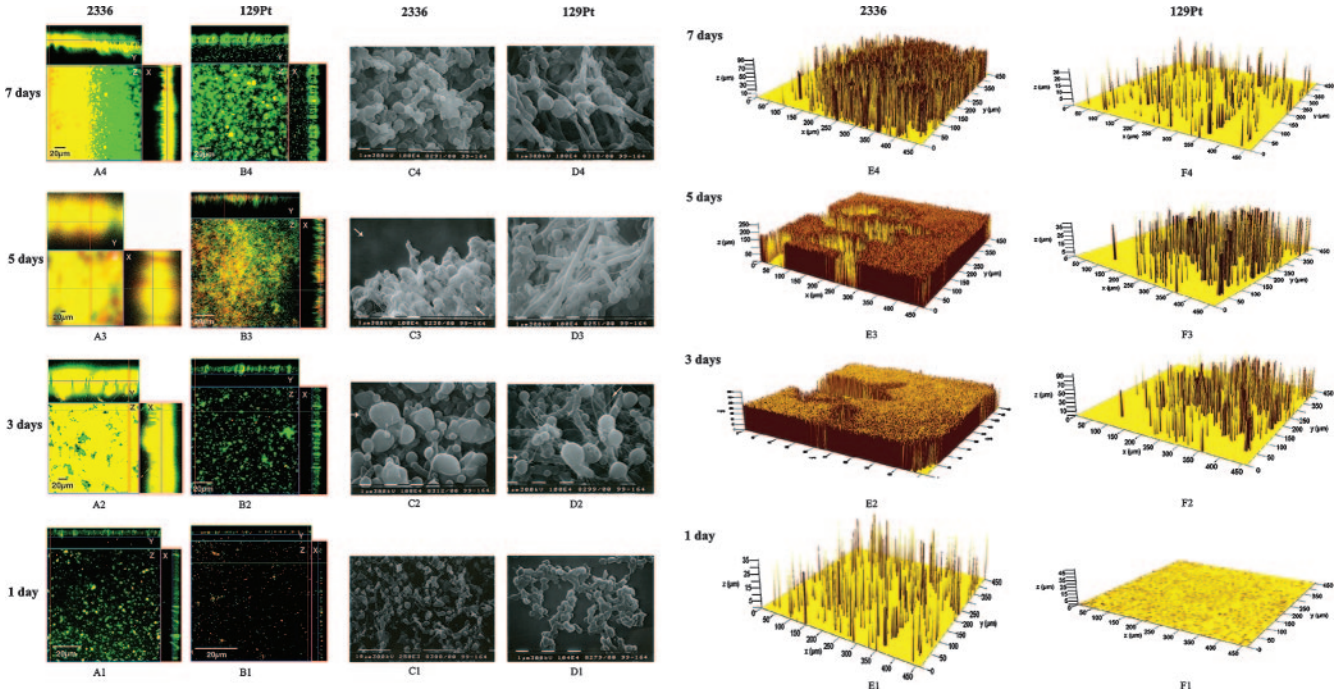

FIG. 2. Comparison of the life cycle of biofilm formation by *H. somni* strains 2336 and 129Pt. Orthogonal sections showing horizontal (*z*) and side views (*x* and *y*) of reconstructed three-dimensional biofilm images at a magnification of ×20. Biofilms were stained with LIVE/DEAD stain, resulting in live and dead bacteria appearing as green or red, respectively. Panels A1 to D1 show the first stage of biofilm formation at day 1, panels A2 to D2 show the second stage of biofilm formation at day 3, panels A3 to D3 show the third stage of biofilm formation at day 5, and panels A4 to D4 show the fourth stage of biofilm formation at day 7. Panels A1 to A4 show confocal images of biofilm formation by strain 2336 at 1, 3, 5, and 7 days of growth, respectively, and panels B1 to B4 show confocal images of biofilm formation by strain 129Pt at 1, 3, 5, and 7 days of growth, respectively. Dead organisms appear red, live organisms appear green, and a mixture of live and dead organisms appear yellow. Panels C1 to C4 show SEM images of biofilm formation by strain 2336 at 1, 3, 5, and 7 days of growth, respectively, and panels D1 to D4 show SEM images of biofilm formation by strain 129Pt at 1, 3, 5, and 7 days of growth, respectively. Arrows indicate (i) microcolonies in the biofilms of strain 2336 (C2) and in strain 129Pt (D2), (ii) exopolysaccharide thin strands in the biofilm of strain 129Pt (D2) and ePS matrix by strain 2336 (C3), and (iii) water channels in the biofilm of strain 2336 (C3). Panels E1 to E4 and F1 to F4 show topographical images of biofilm growth at 1, 3, 5, and 7 days for strains 2336 and 129Pt, respectively.

oped at the substratum, which was reflected by an increase in the substratum coverage, mean thickness, and biomass, and subsequent decrease in the surface/volume ratio. The biofilm of strain 2336 has a biomass of 130 to 168 $\mu m^3/\mu m^2$, mean thickness of 150 to 180 μm and substratum coverage of 81, and a surface/volume ratio of 0.12 $\mu m^2/\mu m^3$. In contrast, the biofilm of strain 129Pt has a biomass of 18 to 20 $\mu m^3/\mu m^2$, mean thickness of 15 to 20 μm, substratum coverage of 14.7, and a surface/volume ratio of 1.56 $\mu m^2/\mu m^3$.

At day 5, the biofilm of strain 2336 contained larger microcolonies that took the shape of a mound, as reflected by a decrease in substratum coverage, an increase in the surface/volume ratio, and a greater mean thickness and biomass. However, the biofilm of strain 129Pt consisted of cell clusters and long filaments with a maximum thickness of 90 μm, resulting in an increase in substratum coverage and a decrease in surface/volume ratio. However, the biofilm of strain 2336 had significantly greater biomass (200 $\mu m^3/\mu m^2$; $P = 0.04$) and thickness (250 to 300 μm; $P = 0.03$), compared to the biomass (30 to 40 $\mu m^3/\mu m^2$) and thickness (80 to 90 μm) of strain 129Pt.

At day 7, the biofilm of strains 2336 and 129Pt became flat and unstructured, as indicated by a decrease in substratum coverage, mean thickness, and biomass. The biofilm of strain 2336 underwent a remarkable decrease in biomass and thickness, which diminished from 200 $\mu m^3/\mu m^2$ to 50 $\mu m^3/\mu m^2$ and from 250 μm to 60 μm, respectively. In a similar manner, the biofilm of strain 129Pt decreased in biomass and thickness from 40 $\mu m^3/\mu m^2$ to 5 $\mu m^3/\mu m^2$ and from 50 μm to 7 μm, respectively.

Another parameter that clearly differed in the two strains was the roughness coefficient. A rough biofilm has many pillars and towers of cells separated by areas devoid of cells, whereas a smooth biofilm consists of a more homogenous layer of cells (18). Strain 2336 had a roughness coefficient (*R*) of about 0.1 throughout the growth period of 3, 5, and 7 days, indicating the formation of a homogenous and uniform biofilm. In contrast, strain 129Pt had an *R* of about 2, indicating formation of a rough and heterogeneous biofilm.

In summary, a comparative analysis of the biofilms of strains 2336 and 129Pt for the variables described above indicated that the strains formed significantly different biofilms at all stages (Fig. 3). Comparison of the 5-day-old mature biofilms demonstrated that strain 2336 colonized the large substratum rapidly and formed a thick biofilm characterized by larger microcolonies that were separated by water channels. In contrast, the biofilm of strain 129Pt formed a thin and heterogeneous biofilm characterized by smaller microcolonies with elongated tower-shaped structures.

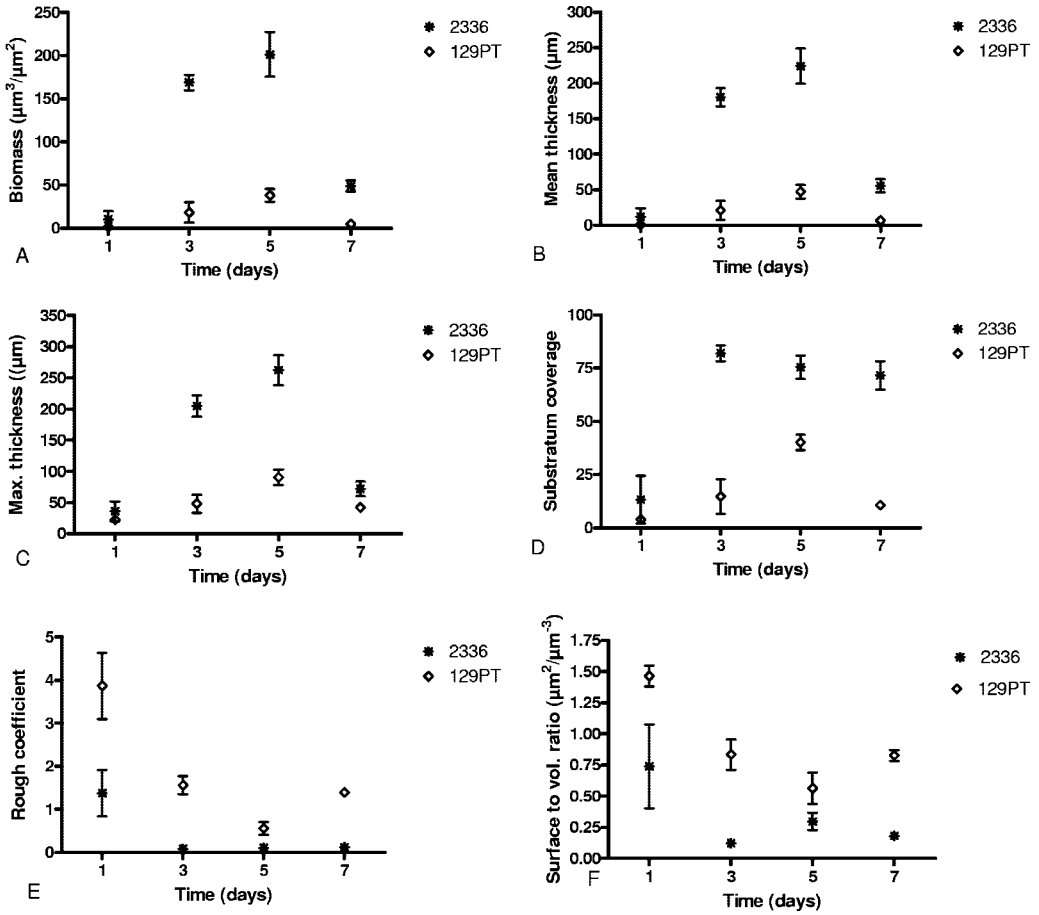

FIG. 3. Comparison of different variables for biofilm formation by pathogenic strain 2336 and commensal strain 129Pt at 1, 3, 5, and 7 days of growth. Variables examined include biomass (A), mean thickness (B), maximum thickness (C), substratum coverage (D), roughness coefficient (E), and surface/volume ratio (F). Graph lines represent the cumulative data of two independent experiments. Error bars represent the standard deviations.

DISCUSSION

Many members of the *Pasteurellaceae* family such as *Pasteurella* spp. (38), *M. haemolytica* (38), *A. pleuropneumoniae* (31), *H. parasuis* (28), *A. actinomycetemcomitans* (30), and *H. influenzae* (15, 35, 45) have been reported to form biofilms. *P. multocida* requires special growth conditions, such as the addition of fetal bovine serum, incubation under 10% CO_2, and a longer culture time to form a biofilm in the Calgary Biofilm Device (38). *H. somni* did not require any special conditions to form a biofilm, which developed in all media tested. Only some strains of *A. pleuropneumoniae* form biofilms in microtiter plates or glass tubes with agitation, and the phenotype of the biofilm is lost when the bacteria are passed two times in broth (31). In the present study of the *A. pleuropneumoniae* strains tested, only strain K17 serotype 5 formed a biofilm in PVC wells. For *H. parasuis*, most strains form a biofilm in vitro, but the phenotype of biofilm formation is related to the in vivo recovery site of the strain (28). However, in the present study *H. parasuis* strain 8869/92 did not form a biofilm in PVC wells. In contrast, all strains of *H. somni* tested formed a biofilm based on the ring assay for microbial deposit on PVC wells (10). Of particular interest was that *H. somni* formed a biofilm within 48 h under most types of growth conditions in broth, except during rapid shaking (~200 rpm). However, the biofilm formed by a pathogenic strain of *H. somni* was very different from that of a commensal strain. Although other strains were not examined in detail, based on the greater amount of biofilm formed by most pathogenic strains compared to commensal strains in PVC wells, the differences in biofilm biomass and structures observed are likely to be consistent. It is possible that there are phylogenetic differences between pathogenic and commensal strains of *H. somni*, which could correlate with differences in biofilm architecture. The 16S rRNA gene sequence is highly similar between all *H. somni* strains (>99.5%). However, greater heterogeneity and resolving power exists in the *rpoB* gene sequence (3). Further investigation is required in order to determine whether pathogenic and commensal isolates can be clustered based on the sequence of the *rpoB* gene, and if this gene plays a role in biofilm formation.

A unique feature of *H. somni* that distinguishes it from other members of the *Pasteurellaceae* is the substantial difference in the amount and architecture of biofilm formed by pathogenic strains compared to commensal strains. Biofilm development in many bacterial species progresses through multiple devel-

opmental stages (9, 10, 40, 41, 50). We demonstrated that biofilm formation in *H. somni* displayed a distinct, phenotypic life cycle that also went through progressive stages of attachment, growth, maturation, and detachment. *A. actinomycetemcomitans* forms a biofilm that also exhibits a distinct, phenotypic life cycle characterized by adherence of planktonic cells to a surface, growth of asymmetric, lobed microcolonies that display complex morphological features, and the subsequent release of cells from the biofilm colony (30). Of note was that the biofilm structures of pathogenic and commensal strains of *H. somni* were distinct, based on CLSM, SEM, and quantification of the biofilms using COMSTAT software. Clinical isolates of nontypeable *H. influenzae* from the middle ear of children with otitis media and from the sputum of adults with chronic obstructive pulmonary disease showed striking differences in their propensity to grow as biofilms in vitro (35). However, detailed studies comparing the biofilm architecture and development of these clinical isolates have not been reported. Mature biofilm structures formed by *Streptococcus pneumoniae* clinical isolates also differ from each other in microcolony size, overall biomass, and biofilm thickness (1). Tolker-Nielsen et al. (49) noted variation in biofilm development by *Pseudomonas* sp. strain B13 and *P. putida* OUS82. Both strains form flat microcolonies initially, but in the later phase of biofilm formation strain B13 forms ball-shaped microcolonies, whereas *P. putida* OUS82 forms loose protruding structures. However, the explanation for such differences in the behavior of biofilm formation by these two pseudomonads is unclear.

A comparative analysis of formation and development of monospecies biofilms by *Pseudomonas putida*, *P. aureofaciens*, *P. fluorescens*, and *P. aeruginosa* was shown using the COMSTAT software, which incorporates 10 features for quantitative characterization of three-dimensional biofilm images (18). Similar software was used in the present study to compare the biofilm architecture and development of *H. somni* pathogenic strain 2336 and commensal strain 129Pt. Strain 2336 formed a biofilm with a high substratum coverage (80 to 85%), a low roughness coefficients of 0.1, and fairly low surface/volume ratios, indicating that it formed a flat uniform biofilm similar to *P. aeruginosa* when citrate was used as the carbon source (16–18). Unlike *P. aeruginosa*, *H. somni* strain 2336 (like *P. aureofaciens*) never obtained 100% substratum coverage at any time point in biofilm formation (18), indicating it had a tendency to form microcolonies. This may be why in later stages of biofilm formation *H. somni* strain 2336 formed thick, mound-shaped microcolonies separated by pronounced water channels. The architecture and shape of the biofilm formed by strain 129Pt was distinct from that of strain 2336. Strain 129Pt formed a thin, heterogeneous, and filament-shaped biofilm with some resemblance to the biofilm of *P. putida* (18).

In conclusion, we have demonstrated the development and architecture of biofilms by two different strains of *H. somni*. The differences in biofilm architecture by the two strains may correlate with pathogenicity, since pneumonia isolate strain 2336 formed significantly larger amounts of biofilm than did commensal strain 129Pt. Since *H. somni* is an obligate inhabitant of bovines, the formation of such a prominent biofilm suggests that this structure may be important for colonization of the respiratory tract, virulence, or both in the host. In contrast, strain 129Pt and other commensal strains need only to colonize the urogenital tract, which is a substantially different environment from that of systemic tissue sites. The genome sequences of strains 2336 and 129Pt have been completed (4, 45) and show there are substantial gene rearrangements and loss or interruption of many genes in strain 129Pt compared to strain 2336. Future microarray analysis is expected to provide additional information regarding the genes that contribute to biofilm formation and differences in biofilm architecture. To further investigate the relationship between biofilm formation and pathogenesis, studies on biofilm formation are under way in the natural host.

ACKNOWLEDGMENTS

We are grateful to Satish Annadata, Gretchen Berg, and Kristen McKeon for technical assistance; Ken Grant for assistance with electron microscopy; and Terry Lawrence for valuable help in graphic design and illustrations.

This study was supported, in part, by USDA/CSREES grants 2001-52100-11314 and 2003-35204-13637 to T.J.I. and NIH grants AI054425 and DC007444 to W.E.S.

REFERENCES

1. **Allegrucci, M., F. Z. Hu, K. Shen, J. Hayes, G. D. Ehrlich, J. C. Post, and K. Sauer.** 2006. Phenotypic characterization of *Streptococcus pneumoniae* biofilm development. J. Bacteriol. **188:**2325–2335.
2. **Andrews, J. J., T. D. Anderson, L. N. Slife, and G. W. Stevenson.** 1985. Microscopic lesions associated with the isolation of *Haemophilus somnus* from pneumonic bovine lungs. Vet. Pathol. **22:**131–136.
3. **Angen, O., P. Ahrens, P. Kuhnert, H. Christensen, and R. Mutters.** 2003. Proposal of *Histophilus somni* gen. nov., sp. nov. for the three species incertae sedis "*Haemophilus somnus*," "*Haemophilus agni*," and "*Histophilus ovis*." Int. J. Syst. Evol. Microbiol. **53:**1449–1456.
4. **Challacombe, J. F., A. J. Duncan, T. S. Brettin, D. Bruce, O. Chertkov, J. C. Detter, C. S. Han, M. Misra, P. Richardson, R. Tapia, N. Thayer, G. Xie, and T. J. Inzana.** 2007. Complete genome sequence of *Haemophilus somnus* (*Histophilus somni*) strain 129Pt and comparison to *Haemophilus ducreyi* 35000HP and *Haemophilus influenzae*. Rd. J. Bacteriol. **189:**1890–1898.
5. **Corbeil, L. B., F. D. Bastida-Corcuera, and T. J. Beveridge.** 1997. *Haemophilus somnus* immunoglobulin binding proteins and surface fibrils. Infect. Immun. **65:**4250–4257.
6. **Corbeil, L. B., K. Blau, D. J. Prieur, and A. C. Ward.** 1985. Serum susceptibility of *Haemophilus somnus* from bovine clinical cases and carriers J. Clin. Microbiol. **22:**192–198.
7. **Corbeil, L. B., P. R. Widders, R. Gogolewski, J. Arthur, T. J. Inzana, and A. C. Ward.** 1986. *Haemophilus somnus*: bovine reproductive and respiratory disease. Can. Vet. J. **27:**90–93.
8. **Czuprynski, C. J., and H. L. Hamilton.** 1985. Bovine neutrophils ingest but do not kill *Haemophilus somnus* in vitro. Infect. Immun. **50:**431–436.
9. **Davey, M. E., and A. G. O'Toole.** 2000. Microbial biofilms: from ecology to molecular genetics. Microbiol. Mol. Biol. Rev. **64:**847–867.
10. **Davies, D. G., and G. G. Geesey.** 1995. Regulation of the alginate biosynthesis gene *algC* in *Pseudomonas aeruginosa* during biofilm development in continuous culture. Appl. Environ. Microbiol. **61:**860–867.
11. **Donlan, R. M., and J. W. Costerton.** 2002. Biofilms: survival mechanisms of clinically relevant microorganisms Clin. Microbiol. Rev. **15:**167–193.
12. **Duncan, A. J., A. Gillaspy, M. Carson, J. Orvis, J. Zaitshik, J. Gipson, M. Gipson, G. Barnes, A. Hendrickson, J. F. Challacombe, T. Brettin, D. W. Dyer, and T. J. Inzana.** 2006. The genome sequence of *Histophilus somni* strain 2336. USDA/NSF Joint Microbial Genome Sequencing Program: Plant And Animal Genomes XIV, San Diego, CA.
13. **Frank, G. H.** 1984. Bacteria as etiologic agents in bovine respiratory disease, p. 347–362. *In* L. R. W. (ed.), Bovine respiratory disease: a symposium. Texas A&M University Press, College Station.
14. **Fussing, V., and H. C. Wegener.** 1993. Characterization of bovine *Haemophilus somnus* by biotyping, plasmid profiling, REA-patterns, and ribotyping. Zentbl. Bakteriol. **279:**60–74.
15. **Greiner, L. L., H. Watanabe, N. J. Phillips, J. Shao, A. Morgan, A. Zaleski, B. W. Gibson, and M. A. Apicella.** 2004. Nontypeable *Haemophilus influenzae* strain 2019 produces a biofilm containing *N*-acetylneuraminic acid that may mimic sialylated O-linked glycans. Infect. Immun. **72:**4249–4260.
16. **Heydorn, A., B. Ersboll, J. Kato, M. Hentzer, M. R. Parsek, T. Tolker-Nielsen, M. Givskov, and S. Molin.** 2002. Statistical analysis of *Pseudomonas aeruginosa* biofilm development: impact of mutations in genes involved in twitching motility, cell-to-cell signaling, and stationary-phase sigma factor expression. Appl. Environ. Microbiol. **68:**2008–2017.

17. **Heydorn, A., B. K. Ersboll, M. Hentzer, M. R. Parsek, M. Givskov, and S. Molin.** 2000. Experimental reproducibility in flow-chamber biofilms. Microbiology **146:**2409–2415.
18. **Heydorn, A., A. T. Nielsen, M. Hentzer, C. Sternberg, M. Givskov, B. K. Ersboll, and S. Molin.** 2000. Quantification of biofilm structures by the novel computer program COMSTAT. Microbiology **146:**2395–2407.
19. **Hong, W., K. Mason, J. Jurcisek, L. Novotny, L. O. Bakaletz, and W. E. Swords.** 2007. Phosphorylcholine decreases early inflammation and promotes the establishment of stable biofilm communities of nontypeable *Haemophilus influenzae* strain 86-028NP in a chinchilla model of otitis media. Infect. Immun. **75:**958–965.
20. **Howard, M. D., A. D. Cox, J. N. Weiser, G. G. Schurig, and T. J. Inzana.** 2000. Antigenic diversity of *Haemophilus somnus* lipooligosaccharide: phase-variable accessibility of the phosphorylcholine epitope. J. Clin. Microbiol. **38:**4412–4419.
21. **Humphrey, J. D., and L. R. Stephens.** 1983. *Haemophilus somnus*: a review. Vet. Bull. **53:**987–1004.
22. **Inzana, T. J., and L. B. Corbeil.** 2004. *Haemophilus*, p. 243–257. *In* C. Gyles, C. Thoen, J. Prescott, and G. Songer (ed.), Pathogenesis of bacterial infections in animals, 3rd ed. Blackwell Publishing, Ltd., Oxford, England.
23. **Inzana, T. J., and L. B. Corbeil.** 1987. Development of a defined medium for *Haemophilus somnus* isolated from cattle. Am. J. Vet. Res. **48:**366–369.
24. **Inzana, T. J., G. Glindemann, A. D. Cox, W. Wakarchuk, and M. D. Howard.** 2002. Incorporation of *N*-acetylneuraminic acid into *Haemophilus somnus* lipooligosaccharide (LOS): enhancement of resistance to serum and reduction of LOS antibody binding. Infect. Immun. **70:**4870–4879.
25. **Inzana, T. J., R. P. Gogolewski, and L. B. Corbeil.** 1992. Phenotypic phase variation in *Haemophilus somnus* lipooligosaccharide during bovine pneumonia and after in vitro passage. Infect. Immun. **60:**2943–2951.
26. **Inzana, T. J., J. Ma, T. Workman, R. P. Gogolewski, and P. Anderson.** 1988. Virulence properties and protective efficacy of the capsular polymer of *Haemophilus* (*Actinobacillus*) *pleuropneumoniae* serotype 5. Infect. Immun. **56:** 1880–1889.
27. **Inzana, T. J., J. Todd, and H. P. Veit.** 1993. Safety, stability, and efficacy of noncapsulated mutants of *Actinobacillus pleuropneumoniae* for use in live vaccines. Infect. Immun. **61:**1682–1686.
28. **Jin, H., R. Zhou, M. Kang, R. Luo, X. Cai, and H. Chen.** 2006. Biofilm formation by field isolates and reference strains of *Haemophilus parasuis*. Vet. Microbiol. **118:**117–123.
29. **Jurcisek, J. A., and L. O. Bakaletz.** 2007. Biofilms formed by nontypeable *Haemophilus influenzae* in vivo contain both double-stranded DNA and type IV pilin protein. J. Bacteriol. **189:**3868–3875.
30. **Kaplan, J. B., M. F. Meyenhofer, and D. H. Fine.** 2003. Biofilm growth and detachment of *Actinobacillus actinomycetemcomitans*. J. Bacteriol. **185:**1399–1404.
31. **Kaplan, J. B., and M. H. Mulks.** 2005. Biofilm formation is prevalent among field isolates of *Actinobacillus pleuropneumoniae*. Vet. Microbiol. **108:**89–94.
32. **Kilian, M.** 2005. Genus III. *Haemophilus*, p. 883–904. *In* D. J. Brenner, N. R. Krieg, J. T. Staley, and G. M. Garrity (ed.), Bergey's manual of systematic bacteriology, 2nd ed. Springer, New York, NY.
33. **Lederer, J. A., J. F. Brown, and C. J. Czuprynski.** 1987. "*Haemophilus somnus*," a facultative intracellular pathogen of bovine mononuclear phagocytes. Infect. Immun. **55:**381–387.
34. **Martin, S. W., R. J. Harland, K. G. Bateman, and E. Nagy.** 1998. The association of titers to *Haemophilus somnus*, and other putative pathogens, with the occurrence of bovine respiratory disease and weight gain in feedlot calves. Can. J. Vet. Res. **62:**262–267.
35. **Murphy, T. F., and C. Kirkham.** 2002. Biofilm formation by nontypeable *Haemophilus influenzae*: strain variability, outer membrane antigen expression and role of pili. BMC Microbiol. **2:**7.
36. **Mutters, R., H. Christensen, and L. Pasteur.** 2005. Genus I. *Pasteurella*, p. 857–866. *In* D. J. Brenner, N. R. Krieg, J. T. Staley, and G. M. Garrity (ed.), Bergey's manual of systematic bacteriology, 2nd ed. Springer, New York, NY.
37. **Olsen, I., and K. Moller.** 2005. Genus II. *Actinobacillus*, p. 866–883. *In* D. J. Brenner, N. R. Krieg, J. T. Staley, and G. M. Garrity (ed.), Bergey's manual of systematic bacteriology, 2nd ed. Springer, New York, NY.
38. **Olson, M. E., H. Ceri, D. W. Morck, A. G. Buret, and R. R. Read.** 2002. Biofilm bacteria: formation and comparative susceptibility to antibiotics. Can. J. Vet. Res. **66:**86–92.
39. **Reysenbach, A. L., and S. L. Cady.** 2001. Microbiology of ancient and modern hydrothermal systems. Trends Microbiol. **9:**79–86.
40. **Sauer, K., A. K. Camper, G. D. Ehrlich, J. W. Costerton, and D. G. Davies.** 2002. *Pseudomonas aeruginosa* displays multiple phenotypes during development as a biofilm. J. Bacteriol. **184:**1140–1154.
41. **Schembri, M. A., K. Kjaergaard, and P. Klemm.** 2003. Global gene expression in *Escherichia coli* biofilms. Mol. Microbiol. **48:**253–2567.
42. **Siddaramappa, S. S., A. J. Duncan, J. F. Challacombe, D. Dyer, A. Gillaspy, J. Gipson, J. Z. M. Carson, D. Rainey, and T. J. Inzana.** 2007. Comparative genomics of *Histophilus somni* strains 2336 and 129pt, Abstr. Microbial Genome 2007, p. 22. The Wellcome Trust, Hinxton, Cambridge, United Kingdom.
43. **Siddaramppa, S., and T. J. Inzana.** 2004. *Haemophilus somnus* virulence factors and resistance to host immunity. Anim. Health Res. Rev. **5:**79–93.
44. **Stoodley, P., K. Sauer, D. G. Davies, and J. W. Costerton.** 2002. Biofilms as complex differentiated communities. Annu. Rev. Microbiol. **56:**187–209.
45. **Swords, W. E., M. L. Moore, L. Godzicki, G. Bukofzer, M. J. Mitten, and J. VonCannon.** 2004. Sialylation of lipooligosaccharides promotes biofilm formation by nontypeable *Haemophilus influenzae*. Infect. Immun. **72:**106–113.
46. **Sylte, M. J., C. J. Kuckleburg, D. Atapattu, F. P. Leite, D. McClenahan, T. J. Inzana, and C. J. Czuprynski.** 2005. Signaling through interleukin-1 type 1 receptor diminishes *Haemophilus somnus* lipooligosaccharide-mediated apoptosis of endothelial cells. Microb. Pathog. **39:**121–130.
47. **Sylte, M. J., C. J. Kuckleburg, T. J. Inzana, P. J. Bertics, and C. J. Czuprynski.** 2005. Stimulation of P2X receptors enhances lipooligosaccharide-mediated apoptosis of endothelial cells. J. Leukoc. Biol. **77:**958–965.
48. **Tegtmeier, C., O. Angen, and P. Ahrens.** 2000. Comparison of bacterial cultivation, PCR, in situ hybridization and immunohistochemistry as tools for diagnosis of *Haemophilus somnus* pneumonia in cattle. Vet. Microbiol. **76:**385–394.
49. **Tolker-Nielsen, T., U. C. Brinch, P. C. Ragas, J. B. Andersen, C. S. Jacobsen, and S. Molin.** 2000. Development and dynamics of *Pseudomonas* sp. biofilms. J. Bacteriol. **182:**6482–6489.
50. **Whiteley, M., M. G. Bangera, R. E. Bumgarner, M. R. Parsek, G. M. Teitzel, S. Lory, and E. P. Greenberg.** 2001. Gene expression in *Pseudomonas aeruginosa* biofilms. Nature **413:**860–864.
51. **Widders, P. R., L. A. Dorrance, M. Yarnall, and L. B. Corbeil.** 1989. Immunoglobulin-binding activity among pathogenic and carrier isolates of *Haemophilus somnus*. Infect. Immun. **57:**639–642.
52. **Wu, Y., J. H. McQuiston, A. Cox, T. D. Pack, and T. J. Inzana.** 2000. Molecular cloning and mutagenesis of a DNA locus involved in lipooligosaccharide biosynthesis in *Haemophilus somnus*. Infect. Immun. **68:**310–319.